ISSN 1330-3651 (Print), ISSN 1848-6339 (Online)
https://doi.org/10.17559/TV-20220408155435
Original scientific paper

Relation between Kinetic Friction Coefficient and Angular Acceleration during Motion Initiated by Dynamic Impact Force

Ljiljana BRZAKOVIC, Vladimir MILOVANOVIC, Vladimir KOCOVIC*, Goran SIMUNOVIC, Djordje VUKELIC, Branko TADIC

Abstract: The paper presents theoretical and experimental analyses of the kinetic friction coefficient of a ball bearing in conditions of rotational motion initiated by dynamic impact force. A method has been developed and a measurement system allows the measurement of a kinetic coefficient of friction through the measurement of the angular acceleration. This paper considers the friction caused by rotational motion initiated by the force impact impulse. After the external force (impact impulse) stops acting, the motion continues, and the loaded bearing (i.e. the zone of the bearing in which the frictional resistance forces act) exhibits a broad spectrum of velocities, from the maximum value at the moment of motion initiation to the zero value when motion stops, where the whole measuring system acts as a rotary encoder. Experimental results indicate a high dependency between angular velocity and friction coefficient, similar to functional dependency. This paper proves that kinetic friction coefficient can be reliably measured using the measurements of angle change and angular velocity. Analysed method has high potential in the diagnostics of energy loss in the tribo-mechanical systems.

Keywords: acceleration; energy; friction; impact

1 INTRODUCTION

The first published theoretical research related to the determination of kinetic friction coefficient using the dynamic equation of motion for a body moving down an inclined plane was published by Euler in 1748 [1]. In the paper "On the friction of solid bodies" [2], Euler analysed the motion and expressed the coefficient of friction as a function of time. His approach enables the determination of the kinetic coefficient of friction based on experimental measurements. Unfortunately, this method has not experienced a broader expansion in the scientific field, especially in the design of modern tribodiagnostic equipment.

Papers based on (or related to) Euler's research are mainly published in journals regarding physics education [3-5]. For example, Alam et al. [6] deals with the dynamics of rotational motion, developing a simple method for experimental determination of friction losses. Applying the relations between translational and rotational motion, they indicated a linear dependence of the friction losses, i.e. the moment of friction, on the angular velocity. Drosd and Minkin [7] also used a simple laboratory device to study the effects of friction between two discs coming into contact while one disc rotates. The paper discussed the dependence of kinetic friction coefficient on the stationary disk radius, gravitational acceleration, and angular acceleration of the disk. Sari [8] designed an Arduino-based experiment to examine the sliding motion of the object on an inclined plane. The acceleration and the kinetic friction coefficient were determined. Siretean et al. [9] proposed a device for finding the coefficient of rolling friction using a sphere in contact with the inner surface of a ring that rotates about a horizontal axis. The nonlinear differential equation of motion was obtained for the intended dynamic model. The oscillatory motion of the ball and the eccentric equilibrium position have been confirmed, and a dependency of equilibrium position on the coefficient of rolling friction has been found. Marques et al. [10] discussed the modelling of frictional effects in the context of multibody dynamics formulation. The example considered the impact motion of a simple journal - bearing system. A static friction model was the most suitable choice for modelling friction since it captures the most relevant friction characteristics, requires a small number of parameters and does not significantly increase the computational time. On the other hand, a dynamic model helps capture some more detailed phenomena, such as frictional lag or pre-sliding displacement. Harris [11] developed a prediction method considering elastohydrodynamic lubrication. The effects of the bearing load, inner ring speed, and the number of rolling elements on skidding of bearing were analysed. Jones [12] proposed a mathematical model to calculate the motion of the bearing. This theory was appropriate for the highspeed bearing with a larger friction coefficient. Sopanen and Mikkola [13, 14] proposed a dynamics model of a deep-groove ball bearing, including the effect of a defect. Nakhaeinejad et al. [15] developed a planar dynamics model of bearing to analyse the dynamic responses of healthy or faulty bearings. Laniado-Jacome et al. [16] discussed the skidding behavior of bearing by using the finite element method. Shao et al. [17] established a bearing finite element model to investigate fault vibration characteristics by seeding small defects at inner race, outer race, and balls, respectively. The results indicated that the vibration response excited by the defect at the outer race was most intensive.

In the paper related to the microhardness test, Deng et al. [18] provided a diagram of changes in friction coefficient as a function of normal load and sliding duration. Their results indicate that, under different contact conditions, the friction coefficient increases with decreasing normal load and increasing the number of load change cycles. Results of the research related to the slippage effect on wear loss induced by the rolling sliding friction [19] show the variation in the friction coefficient curves for three typical slippages at different friction cycles. Under 0,17% slippage, the friction coefficient remained at a low, stable value. However, the friction coefficient value gradually increased to a high value when the slippage increased, with some fluctuation. Results also indicated that the cycle parameters have a negligible effect on the contact state during the friction process. The paper [20] proposed high-frequency vibration to mitigate the effects of pre-rolling/pre-sliding friction on the settling

time of rolling bearing nanopositioning stages. The proposed method resulted in a 52% reduction in mean settling time, i.e. the time needed to reach the target positions in point-to-point positioning tasks, which would otherwise be significantly prolonged due to pre-rolling/pre-sliding friction. This research indicates the complexity of the friction phenomenon and the need to manage friction in an industrial environment. Duan et al. [21] established a new static mechanical model to study the rolling-sliding contact in the real-time non-clearance precision ball drive, using the coupling coefficient determined by the Carter narrow theory. The diagrams of mechanical and geometric parameters simulated by the finite element method indicate that the trend of change in normal load has the shape of a sine function. It should be noted that the value of the friction coefficient in [21] is taken as a constant computer-simulated value. At the same time, in this paper, the normal load of a bearing, achieved by a rotating mass, is an actual constant value, which could not be said for the kinetic coefficient of friction. Namely, depending on the contact conditions, the kinetic coefficient of friction oscillates over time around the dynamic trend. Hu et al. [22] analysed the rolling friction performance of hollow spherical nano-MoS_2/nano-TiO_2 (HSMT) and its conversion from lubricant to photocatalyst. In all experiments, values of friction coefficient ranged from 0,02 to 0,05. The friction coefficient values presented in this paper were obtained at normal contact load of 21,5 N and rolling velocities ranging from 0,03 to 0,06, not exceeding 0,1 m/s. Considering the test conditions (normal load up to 50 N and rolling velocities up to 0,1 m/s), the obtained results are very compatible with the results obtained by the conventional method [22], both from the aspect of the friction coefficient scattering limits and from the aspect of the dynamics of its change. One of a few papers based on Euler's idea to determine the kinetic friction coefficient using the differential equation of motion was published [23]. In order to study the friction between grains of granular material at motion, Mihajlovic et al. [23] developed a method and physical model of a vibrating platform. They have theoretically and experimentally proven that the coefficient of friction between sand grains and sieve can be reliably determined using the dynamic equation of motion in real operating conditions of the vibrating platform. The obtained results are very compatible with the results obtained by standard and considerably more complex methods. Although based on Euler's approach, the presented research further generalises the application of the method for significantly more complex tribological processes than the study of friction on an inclined plane.

Following Euler's idea, several tribometers intended for the determination of kinetic friction coefficient were realised [23-26]. The published results indicate a great potential for this method in terms of an essential understanding of dynamic processes, friction phenomena, and a wide range of possible applications. Furthermore, the determination of kinetic friction coefficient based on differential equations of motion is, in essence, related to the measurement of three base units of the SI system (mass, time, and length), which is a significant advantage in a theoretical, experimental, and technological sense.

2 METHODOLOGY

Methodology of the determination of the kinetic friction coefficient proposed by this paper is based on the initiation of the motion (of the rotating disk) using active rotational moment acting over a short time interval, as well as on the tracking of the changes in the rotational angle over time. Fig. 1 provides a schematic view of the method. Weight P with mass m freefalls from the height h, hitting a dampener a which absorbs the energy which initiates the rotation of the disk RM with angular velocity ω. Weight P, upon impact, continues the fall along the guide V until its end, where it stops. The rotating disk is connected via ball bearing to the rotational encoder RE which measures the change of the angle φ over time. Rotational disk and the contact zone in which friction is caused passes through an entire spectre of angular velocities, from maximal, initiated by the active moment, to the zero value of angular velocity at the moment when the rotation stops. In this, dynamic, system, the kinetic energy invested at the initiation of the motion is reduced with every moment after the initation of the motion, by the effect of the friction force F_t, until the rotation stops.

Thus, the motion of the body upon the initiation of the motion is based on the accumulated energy, in which case the law of the rotational angle change over time defines the value of the friction force F_t. Motion can be initiated manually, using an electromagnetic coupling, by the impulse of the impacting force, or in some other manner. This paper considers the motion initiated by the impacting force, which is the most complex method of initiation, which is why it is taken into consideration.

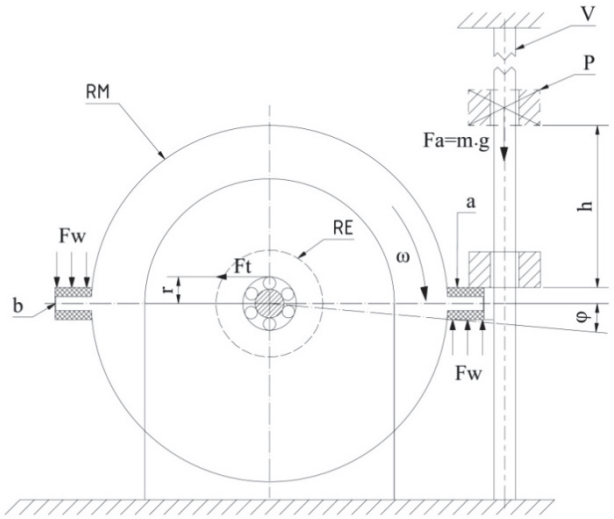

Figure 1 The distribution of active and resistive forces when the body rotates around a fixed axis
(RM - rotating masses, RE - rotary encoder,F_a - impulse impact force,F_w - air resistance force, F_t - resulting friction force at contact, ω - angular velocity,φ - the angle of rotation, h - height, r - radius at which elementary friction forces act, P - pin, V - cylindrical guide)

The method for determining kinetic friction coefficient under dynamic loading conditions is generally based on the differential equation of motion. The following equation describes the motion of a body rotating around a fixed axis (Fig. 1):

$$I\frac{\mathrm{d}\omega}{\mathrm{d}t}=\sum M_i=M_a-M_t-M_w \tag{1}$$

where: I - the mass moment of inertia; ω - angular velocity; M_a - active moment initiating motion; M_t - resulting moment as the integral sum of the resistant moments of friction over the contact surface; M_w - the resulting moment of air resistance.

If the change in the body's rotation angle is determined experimentally as a function of time, then, based on the dynamic equation of motion, it is possible to determine the current values of friction coefficient from the moment of motion initiation to the moment when rotation ends.

After the action of an impulse of a force that initiates the motion in a short time interval Δ_{t1}, from the differential Eq. (1) follows that the active moment equals zero ($M_a = 0$), where $\Delta_{t1} < t$. It means that in the stated time interval ($\Delta_{t1} < t$) the motion continues without the active moment, using the energy accumulated by the moment of impulse.

The air resistance force that creates the moment of resistance M_w can be determined based on the drag coefficient, the rotational velocity, and the size of a surface the air resistance force acts on [26]. Based on the previous research [26], it follows that for the velocity interval $v < 3$ m/s the drag force can be neglected as a lower order quantity, i.e.

$$M_a=0,\ F_w\to 0 \tag{2}$$

Having that in mind, differential Eq. (1) can be written in the following form:

$$I\frac{\mathrm{d}\omega}{\mathrm{d}t}=M_t=F_t r \tag{3}$$

where: M_t - moment of friction; F_t - resulting friction force at contact; r - radius at which elementary friction forces act (Fig. 2).

The resulting moment of friction is the only unknown variable in the differential equation of motion. Based on Fig.1, it is determined by using the expression:

$$M_t=\iint r\mathrm{d}F_t=F_t r \tag{4}$$

which defines the total friction force as an integral sum of elementary friction forces over the contact surface.

Based on the schematic representation provided in Fig. 1, the friction force F_t can be defined as a function of the friction coefficient:

$$\mu=\frac{I\frac{\mathrm{d}\omega}{\mathrm{d}t}}{r\mathrm{g}\left[\Sigma m\right]} \tag{5}$$

where $\sum m$ denotes the sum of all rotating masses loading the bearing, and g denotes the gravitational acceleration.

Based on the known theoretical expressions, the angular velocity and acceleration can be determined by numerical differentiation:

$$\omega=\frac{\mathrm{d}\varphi}{\mathrm{d}t}=\lim_{\Delta t\to 0}\frac{\varphi\left(t+\Delta t\right)-\varphi(t)}{\Delta t} \tag{6}$$

$$\varepsilon=\frac{\mathrm{d}\omega}{\mathrm{d}t}=\lim_{\Delta t\to 0}\frac{\omega\left(t+\Delta t\right)-\omega(t)}{\Delta t} \tag{7}$$

The stated theoretical considerations indicate that experimentally determined change in rotation angle as a function of time enables the determination of kinetic friction coefficient from the moment when the effect of active moment ceases and until the rotating body stops.

3 RESULTS

Experimental validation of the theoretical model was realised on a preliminary device shown in Fig. 2.

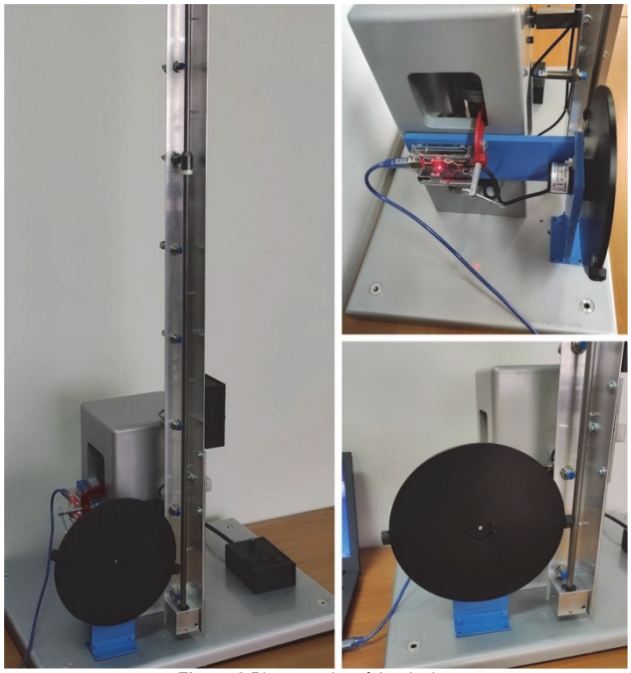

Figure 2 Photographs of the device

The measuring system (rotary encoder), together with accompanying Arduino electronics and developed software, enables the formation of a database, online monitoring of processes, and creation of test reports in tabular and diagrammatic form for different experimental conditions.

A total of 60 experiments were performed. In the first series of 30 experiments, the dynamic loading was initiated by the impulse impact force of a pin weighing 0,0487 kg from a height of 0,21 m. During the second series of 30 experiments, the same mass initiated the dynamic loading but from the height of 1,21 m.

Fig. 3 shows the experimentally obtained changes in the angle and angular velocity increment, angular acceleration and friction coefficient as functions of time during one of 30 experiments in the first series.

For the same experiment, in Fig. 4 are given changes in angular acceleration and a comparative presentation of changes and differences between the experimentally obtained friction coefficient and the friction coefficient determined based on the presented theoretical model.

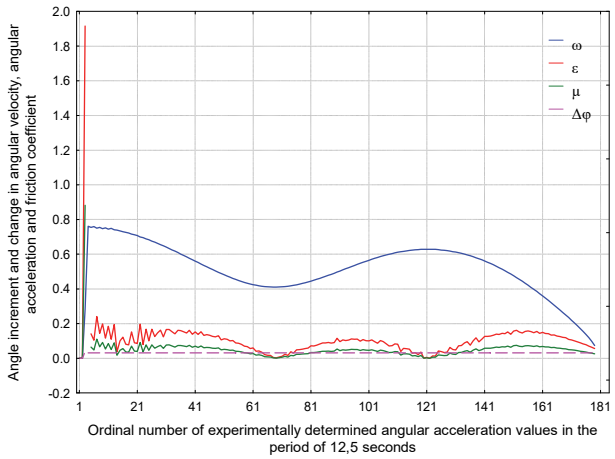

Figure 3 Angle increment ($\Delta\varphi$) and change in angular velocity (ω), angular acceleration (ε) and friction coefficient (μ) determined based on 177 measurements data in the period from the moment of motion initiation to the moment when the rotation ends

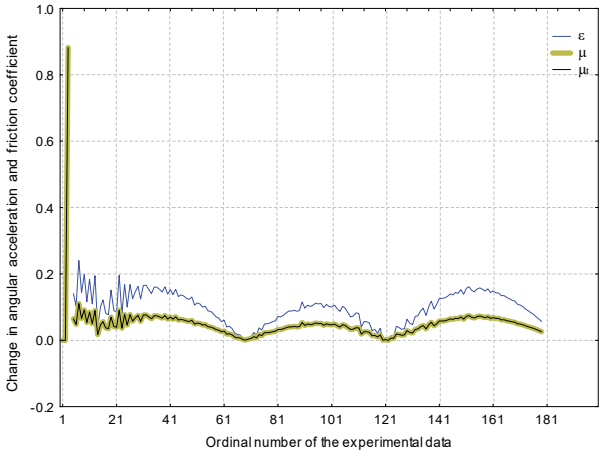

Figure 4 Change in angular acceleration (ε), experimentally determined friction coefficient (μ) and theoretically determined friction coefficient (μ_t) during the period from the motion initiation by the impact impulse to the moment when the rotation ends

The diagram in Fig. 5 refers to the experimental data obtained during one of the 30 experiments performed in the second series. A combined diagram of the increment of angle and angular velocity and the changes in angular acceleration and friction coefficient (Fig. 5) provides a more integrated picture of the process.

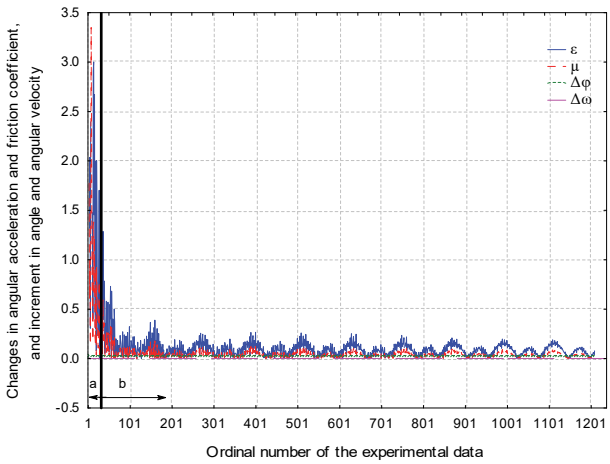

Figure 5 Changes in angular acceleration (ε) and friction coefficient (μ), and increment of angle ($\Delta\varphi$) and angular velocity ($\Delta\omega$) during the motion initiated by impact impulse energy of higher values

High values of friction coefficient (Fig. 5, zone a) are related to the moment of the effect of the active force and active moment which initiate motion. The values of the friction coefficient during the initation of the motion are not relevant and are not considered in this paper. Upon the cessation of the active moment the motion is based on the accumulated energy of the impact (Fig. 5, zone b). The diagramme in the Fig. 5 presents a highlighted border between the time (vertical line) after which the motion and the kinetic friction process act based on the accumulated energy.

The diagram in Fig. 5 indicates that in a short period of time after the motion initiation, the data scattering reduces and increments of angle and angular velocity maintain approximately constant values. Also, the dynamics of the change in angular acceleration and friction coefficient are identical.

Statistical processing of the first series of 30 experimental results confirmed that the theoretical expression for calculating the friction coefficient (Eq. (5)) agrees with the expression obtained by processing experimental data. Namely, the results of statistical data processing define the friction coefficient as a product of a constant and the angular acceleration, i.e.

$$\mu = C\frac{\mathrm{d}\omega}{\mathrm{d}t} \tag{8}$$

where the correlation coefficient equals one ($R = 1$). Also, the experimentally determined constants in all 30 experiments are equal to 0,46073, which is identical to the value of the constant defined by the presented theoretical model (Eq. (5)), i.e.

$$C = \frac{I}{rg\left[\Sigma m\right]} = \frac{0{,}0485875}{0{,}005\cdot 9{,}81\cdot 2{,}15} = 0{,}46073 \tag{9}$$

In the second series of 30 experiments, where the motion was initiated by impulse energy of significantly higher values, deviations of experimentally determined values of constants in relation to the theoretical value of 0,46073 ranged from zero to 5%, with high values of correlation coefficients ($R > 0{,}995$).

Tab. 1 presents the range of the measured output values depending on the free fall height of the body h in the motion zone based on the accumulated impact energy.

Table 1 The range of the measured output values depending on the free fall height of the body h in the motion zone based on the accumulated impact energy

h / m		Δt / s	$\Delta\omega$ / rad/s	ε / rad/s^2	μ
0,21	min	0,03736	0,000168	0,00203	0,00093
	max	0,14508	0,010386	0,26751	0,12325
1,21	min	0,01918	0,000001	0,00005	0,00002
	max	0,04146	0,021788	1,13550	0,52315

Energy balances, i.e. curves of changes in the kinetic energy and energy of friction force work and the differences between these energies, are provided in Figs. 6 and 7. The diagrams were obtained by statistical processing of the results from one of the 30 experiments performed in the first series with lower impact energy and one of the 30 experiments performed in the second series with significantly higher impact energy.

For each of the 184 measurements data from one of the experiments in the first series (Fig. 6) and each of the 1406 measurements data from one of the experiments in the second series (Fig. 7), energies were calculated according to the following expressions:

$$E_k = \frac{1}{2} J \omega^2 \tag{10}$$

$$A_t = E_t = rg\left[\Sigma m\right] \mu \Delta\varphi \tag{11}$$

$$\Delta E = E_k - A_t \tag{12}$$

Here, $\Delta\varphi$ refers to the experimentally determined value of the angle increment as the difference between the $(i + 1)$-th and i-th angle data. Angle change is a constant whose value is equal to $\Delta\varphi$ = 0,03141592 rad. The constants that appear in the expressions above have the following values: J = 0,048587 kgm^2, r = 0,005 m, g = 9,81 m/s^2 and $\sum m$ = 2,15 kg.

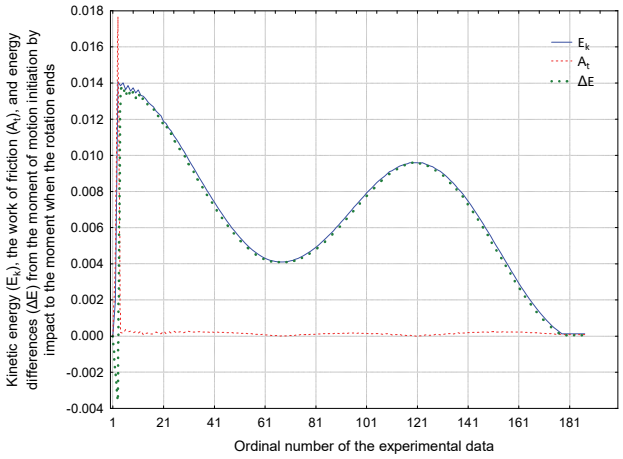

Figure 6 Energy balances at small levels of impact impulse energy

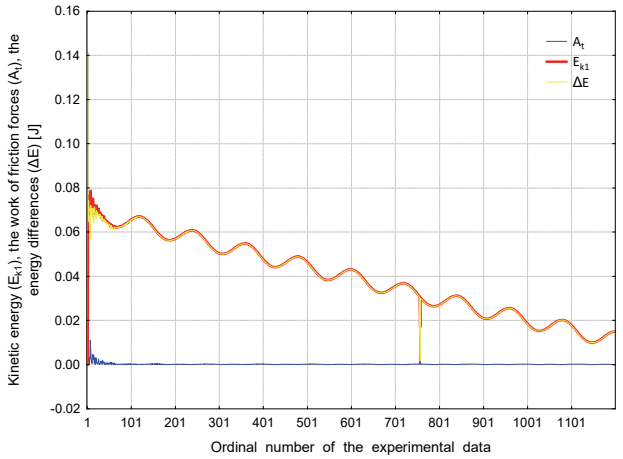

Figure 7 Energy balances at significantly higher levels of impact impulse energy

4 DISCUSSION

The proposed theoretical model for calculating the kinetic friction coefficient agrees with experimentally obtained results presented in the third chapter. The scattering limits of obtained values for rolling friction coefficients (Figs. 3 to 7) correspond to the scattering limits of the results obtained by conventional methods based on the measurement of friction force and contact load [22]. In addition, the measurement repeatability was confirmed through a large number of experiments.

The change dynamics in friction coefficient follow the changes in angular acceleration and indicate the theoretical, experimentally confirmed connection between these quantities (Fig. 4) as a physical law. The energy balance diagrams in Figs. 6 and 7 indicate that the work of friction forces causes a decline in kinetic energy. Accordingly, when the motion ends (Fig. 6), the difference between kinetic energy and friction work is close to zero. The energy balance diagram in Fig. 7 shows that the motion did not stop and that the difference between kinetic energy and friction works is of the order of 0,01 J, which indicates the method's potential in quantifying very small energy losses.

The literature analysis leads to the conclusion that energy losses and friction phenomena are problems of great interest in the field of research and development of modern tribodiagnostic equipment. Tribometry methods for experimental determination of the kinetic friction coefficient are based on the measurement of friction force at certain levels of normal contact load and velocity of one contact element motion relative to another. Other contact conditions (e.g. microgeometry of contact pairs, temperature level in the contact zone, type of lubricant) can vary within wide limits. Literature sources related to the determination of kinetic friction coefficient under dynamic loading conditions [9-22] indicate excellent compatibility of conventional methods with the method presented in this paper. The stated compatibility between the methods follows from comparing the trends in the dynamic of change in friction coefficient and the values of friction coefficients.

5 CONCLUSIONS

Based on the theoretical and experimental research results presented in this paper, it can be concluded that the kinetic friction coefficient can be reliably determined based on the differential equations of motion. The theoretical relation between angular acceleration and coefficient of friction was experimentally verified. Regardless of their amplitude and frequency, changes in acceleration exist in every dynamic system, and they can, to a great extent, explain the enigma of the kinetic friction coefficient. The authors of this paper consider acceleration as a kind of physical and energy indicator of friction and energy dissipation in tribomechanical systems.

The fact that this method is based on the measurement of base physical quantities (time, distance travelled, and angle of rotation) allows the formation of reliable measurement chains and their location outside the contact zone. It considerably simplifies tribological research in the conditions of high-temperature levels, controlled vacuum levels, or aggressive environments.

The high reliability of the results indicates a great potential of the proposed method in the fields of research and development of tribodiagnostic equipment.

The proposed methodology for determining the kinetic coefficient of friction has no essential limitations. The friction coefficient can be determined in any contact

conditions. Sliding and rolling pairs of different tribological characteristics can be tested, where the level of simulated load and the range of sliding or rolling velocities can vary in a wide range. With this method, tests can be performed much simpler than using conventional methods by simulating different levels of contact temperatures and, in general, different conditions that more closely define the operation of real tribomechanical systems (aggressive environment, lubrication system, etc.).

Future research shall be directed towards the application opportunities of the proposed method in the conditions of the dynamic load of the contacts, in which case shall the dynamic load be achieved with the masses position excentrically in relation to the rotation axis, that is, in relation to the inertia forces which theses masses initiate. Also, future research shall be directed in the domain of the motion initation using contactless electromagnetic coupling which will significantly improve the motion initiation system and expand the application range of the proposed method. Future research should focus on implementing the proposed method in tribo-diagnostics of real industrial tribomechanical systems, in terms of quantifying energy losses caused by friction in finished industrial assemblies related to the drive shafts and bearing.

6 REFERENCES

[1] Zhuravlev, V. P. (2013). On the history of the dry friction law. *Mechanics of Solids*, *48*(4), 364-369. https://doi.org/10.3103/S002565441304002X

[2] Euler, L. (1750). Sur le frottement des corps solides. *Memoires de l'academie des sciences de Berlin*, *4*, 122-132. Retrieved from https://scholarlycommons.pacific.edu/euler-works/143/

[3] Maslova, K., De Jesus, V. L. B., & Sasaki, D. G. G. (2020). Understanding the effect of rolling friction in the inclined track experiment. *Physics Education*, *55*(5), 055010. https://doi.org/10.1088/1361-6552/ab9217

[4] Yan, Z., Xia, H., Lan, Y., & Xiao, J. (2017). Variation of the friction coefficient for a cylinder rolling down an inclined board. *Physics Education*, *53*(1), 015011. https://doi.org/10.1088/1361-6552/aa8974

[5] Chakrabarti, S., Khaparde, R. B., & Kachwala, A. H. (2020). Experimental study of the coefficient of rolling friction of the axle of a Maxwell's wheel on a soft horizontal surface. *European Journal of Physics*, *41*(3), 035803. https://doi.org/10.1088/1361-6404/ab78a5

[6] Alam, J., Hassan, H., Shamim, S., Mahmood, W., & Anwar, M. S. (2011). Precise measurement of velocity dependent friction in rotational motion. *European Journal of Physics*, *32*(5), 1367. https://doi.org/10.1088/0143-0807/32/5/024

[7] Drosd, R. & Minkin, L. (2020). Measuring the coefficient of kinetic friction by exploring dynamics of rotational motion. *The Physics Teacher*, *58*(3), 176-178. https://doi.org/10.1119/1.5145409

[8] Sari, U. (2019). Using the Arduino for the experimental determination of a friction coefficient by movement on an inclined plane. *Physics Education*, *54*(3), 035010. https://doi.org/10.1088/1361-6552/ab0919

[9] Siretean, S. T., Muscă, I., Alaci, S., & Ciornei, F.-C. (2018). Use of Hypocycloidal Motion in the Study of Rolling Friction. *Mechanisms and Machine Science*, 467-476. https://doi.org/10.1007/978-3-319-79111-1_46

[10] Marques, F., Flores, P., Claro, J. C. P., & Lankarani, H. M. (2018). Modeling and analysis of friction including rolling effects in multibody dynamics: a review. *Multibody System Dynamics*, *45*(2), 223-244. https://doi.org/10.1007/s11044-018-09640-6

[11] Harris, T. A. (1971). An Analytical Method to Predict Skidding in Thrust-Loaded, Angular-Contact Ball Bearings. *Journal of Lubrication Technology*, *93*(1), 17-23. https://doi.org/10.1115/1.3451511

[12] Jones, A. B. (1960). A General Theory for Elastically Constrained Ball and Radial Roller Bearings under Arbitrary Load and Speed Conditions. *Journal of Basic Engineering*, *82*(2), 309-320. https://doi.org/10.1115/1.3662587

[13] Sopanen, J. & Mikkola, A. (2003). Dynamic model of a deep-groove ball bearing including localised and distributed defects. Part 1: Theory. *Proceedings of the Institution of Mechanical Engineers, Part K: Journal of Multi-Body Dynamics*, *217*(3), 201-211. https://doi.org/10.1243/14644190360713551

[14] Sopanen, J. & Mikkola, A. (2003). Dynamic model of a deep-groove ball bearing including localised and distributed defects. Part 2: Implementation and results. *Proceedings of the Institution of Mechanical Engineers, Part K: Journal of Multi-Body Dynamics*, *217*(3), 213-223. https://doi.org/10.1243/14644190360713560

[15] Nakhaeinejad, M. & Bryant, M. D. (2011). Dynamic Modeling of Rolling Element Bearings with Surface Contact Defects Using Bond Graphs. *Journal of Tribology*, *133*(1). https://doi.org/10.1115/1.4003088

[16] Laniado-Jácome, E., Meneses-Alonso, J., & Diaz-López, V. (2010). A study of sliding between rollers and races in a roller bearing with a numerical model for mechanical event simulations. *Tribology International*, *43*(11), 2175-2182. https://doi.org/10.1016/j.triboint.2010.06.014

[17] Shao, Y., Tu, W., & Gu, F. (October 27-30, 2010). A simulation study of defects in a rolling element bearing using FEA. *International Conference on Control, Automation and Systems (ICCAS 2010)*. https://doi.org/10.1109/iccas.2010.5669813

[18] Deng, G., Tieu, A. K., Su, L., Wang, P., Wang, L., Lan, X., & Zhu, H. (2020). Investigation into reciprocating dry sliding friction and wear properties of bulk CoCrFeNiMo high entropy alloys fabricated by spark plasma sintering and subsequent cold rolling processes: Role of Mo element concentration. *Wear*, *460*, 203440. https://doi.org/10.1016/j.wear.2020.203440

[19] Zhou, Y., Gui, Z. Z., Mo, J. L., Peng, J. F., Xu, Z. B., & Zhu, M. H. (2021). Slippage effects on the crack behavior of pearlitic steel induced via rolling-sliding friction. *Wear*, *482*, 203959. https://doi.org/10.1016/j.wear.2021.203959

[20] Dong, X., Yoon, D., & Okwudire, C. E. (2017). A novel approach for mitigating the effects of pre-rolling/pre-sliding friction on the settling time of rolling bearing nanopositioning stages using high frequency vibration. *Precision Engineering*, *47*, 375-388. https://doi.org/10.1016/j.precisioneng.2016.09.011

[21] Duan, L., An, Z., Yang, R., & Fu, Z. (2016). Mechanical model of coupling rolling and sliding friction in real-time non-clearance precision ball transmission. *Tribology International*, *103*, 218-227. https://doi.org/10.1016/j.triboint.2016.06.032

[22] Hu, K. H., Xu, Y., Hu, E. Z., Guo, J. H., & Hu, X. G. (2016). Rolling friction performance and functional conversion from lubrication to photocatalysis of hollow spherical nano-MoS_2/nano-TiO_2. *Tribology International*, *104*, 131-139. https://doi.org/10.1016/j.triboint.2016.08.029

[23] Mihajlović, G., Gašić, M., Savković, M., Mitrović, S., & Tadić, B. (2017). Vibroplatform modelling with allowance for tribological aspects. *Journal of Friction and Wear*, *38*(3), 184-189. https://doi.org/10.3103/s1068366617030102

[24] Lukovic, M., Miljojkovic, J., & Tadic, B. (2021). An inclined plane based instrument for determining the static

coefficient of friction at high temperatures. *Romanian Journal of Physics*, *66*(9-10), 909.
[25] Miljojković, J., Kočović, V., Luković, M., Živković, A., & Šimunović, K. (2022). Development of a modular didactic laboratory set for the experimental study of friction. *Tehnicki vjesnik - Technical Gazette*, *29*(1), 269-277. https://doi.org/10.17559/TV-20210925171045
[26] Vukelic, D., Todorovic, P., Simunovic, K., Miljojkovic, J., Simunovic, G., Budak, I., & Tadic, B. (2021). A novel method for determination of kinetic friction coefficient using inclined plane. *Tehnicki vjesnik - Technical Gazette*, *28*(2), 447-455.https://doi.org/10.17559/tv-20201101051835

Contact information:

Ljiljana BRZAKOVIC, M.Sc., Teaching Assistant
Academy of Professional Studies Sumadija, Department in Trstenik,
Radoja Krstica 19, 37240 Trstenik, Serbia
E-mail: ljbrzakovic@asss.edu.rs

Vladimir MILOVANOVIC, PhD, Assistant Professor
University of Kragujevac, Faculty of Engineering,
Sestre Janjic 6, 34000 Kragujevac, Serbia
E-mail: vladicka@kg.ac.rs

Vladimir KOCOVIC, PhD, Assistant Professor
(Corresponding author)
University of Kragujevac, Faculty of Engineering,
Sestre Janjic 6, 34000 Kragujevac, Serbia
E-mail: vladimir.kocovic@kg.ac.rs

Goran SIMUNOVIC, PhD, Full Professor
University of Slavonski Brod, Mechanical Engineering Faculty in Slavonski Brod,
Trg Ivane Brlic Mazuranic 2, 35000 Slavonski Brod, Croatia
E-mail: gsimunovic@unisb.hr

Djordje VUKELIC, PhD, Full Professor
University of Novi Sad, Faculty of Technical Sciences,
Trg Dositeja Obradovica 6, 21000 Novi Sad, Serbia
E-mail: vukelic@uns.ac.rs

Branko TADIC, PhD, Full Professor
University of Kragujevac, Faculty of Engineering,
Sestre Janjic 6, 34000 Kragujevac, Serbia
E-mail: btadic@kg.ac.rs